ISSN 0027-1349, Moscow University Physics Bulletin, 2017, Vol. 72, No. 4, pp. 396–401. © Allerton Press, Inc., 2017.
Original Russian Text © M.Yu. Reshetnyak, 2017, published in Vestnik Moskovskogo Universiteta, Seriya 3: Fizika, Astronomiya, 2017, No. 4, pp. 54–59.

ASTRONOMY, ASTROPHYSICS, AND COSMOLOGY

The Equatorial Asymmetry of a Magnetic Field

M. Yu. Reshetnyak[a, b]

[a] *Schmidt Institute of Physics of the Earth, Russian Academy of Sciences, Moscow, 123995 Russia*
[b] *Pushkov Institute of Terrestrial Magnetism, the Ionosphere, and Radio Wave Propagation, Russian Academy of Sciences, Moscow, 142190 Russia*
e-mail: m.reshetnyak@gmail.com

Received May 10, 2016; in final form, November 11, 2016

Abstract—Solution of the inverse problem for Parker's one-dimensional mean-field dynamo model in a thin spherical layer is considered. The method allows the spatial distribution of energy sources, the α- and Ω-effects, to be found provided specified constraints occur on the solution. The highest ratio of the magnetic energies for the Northern and Southern hemispheres is discussed as such a constraint. The method is a modification of the Monte-Carlo technique; it is convenient for parallel computations and based on minimization of the cost function that characterizes the deviation of the model solution properties from the desired ones. The calculations show that the ratio of the energies in the hemispheres may exceed an order of magnitude for both poloidal and toroidal components of the magnetic energy. The ratio depends on the distance of the effective zone of the generation of the magnetic field from the equator and the number of harmonics in the spectrum. The greater this distance is and the higher the number of harmonics is, the stronger the magnetic field asymmetry can be.

Keywords: Parker's model, inverse problem, dynamo theory.
DOI: 10.3103/S0027134917040129

INTRODUCTION

The current dynamo models describe transformation of the kinetic energy of conductive liquid flows to magnetic field energy. The theory can explain the magnetic fields observed in many astrophysical objects, e.g., galaxies, stars, and planets [1, 2]. In dependence on the volume of observations and information available for various objects, the models may differ in complexity. Mean-field models exist that describe the large-scale features of the magnetic field, as well as three-dimensional dynamo models that include the processes of material differentiation, heat exchange, and turbulent effects. Simulations of the dynamo processes make it possible to study new interesting physical effects rather than only selecting the optimal parameters for a particular model. Further, we will focus on analyzing whether the magnetic field can be generated under the conditions that the magnetic energy levels are different in different hemispheres, while there is no asymmetry between the energy sources in the model.

Equatorial asymmetry is well known. In the geomagnetism theory, this asymmetry was explained by superposition of the dipole and quadrupole modes [3]. Since the thresholds of generation of these modes are similar, simultaneous generation will be interpreted as a strong magnetic field in one hemisphere and a weak one in the other. This scenario does not contradict the paleomagnetic observations of the Phanerozoic Eon (560 Myr).

In the solar dynamo, the equatorial asymmetry is present in at least two forms. First, it is the difference between the magnetic fluxes from two hemispheres, so that the sign of this difference may change in time [4]. One more manifestation of the asymmetry occurred during the Maunder minimum in the 17th century, when more than 95% of sunspots were located in the Southern hemisphere of the Sun [5].

Observations of planetary magnetic fields also reveal equatorial asymmetry. A remarkable example is the ancient magnetic field of Mars recorded in the residual magnetization of the crust and associated with the dynamo mechanism that was active in the past [6].

The equatorial asymmetry of the magnetic field does not contradict the dynamo theory and is present in numerical models. With some particular sets of parameters, such phenomena can be reproduced in three-dimensional dynamo simulations in a spherical shell, including the thermal convection equations under the Boussinesq approximation with spherically symmetrical boundary conditions [7–9]. It is interesting to note that in the considered models the distribution of the kinetic energy exhibited substantially

weaker equatorial asymmetry, if any, than that of the magnetic energy.

For the case where the equatorial asymmetry of flows in the convective zones could be caused by the processes in the mantles of the planets, deviations of the thermal flux at the outer boundary from spherical symmetry were introduced into the three-dimensional models [6, 10, 11], which also induced the emergence of the equatorial asymmetry in the magnetic field.

Below, based on the example of a simple mean-field dynamo model, we will consider whether a magnetic field with a high degree of equatorial asymmetry can be generated if the energy sources exhibit no asymmetry. Since the behavior of Parker's nonlinear one-dimensional model considered here may be rather complex, the spatial distributions of the energy sources from which the maximum asymmetry of the magnetic field can be obtained will be determined in the inverse problem solution. The used method for solving the inverse problem, which was first adapted for the Parker equations in [12], makes it possible to select the most significant factors that cause the specified behavior of the magnetic field. The method can easily be modified for a wide class of nonlinear problems of mathematical physics of a high spatial and parametric dimension.

1. A DYNAMO IN A SPHERICAL SHELL

Generation of a magnetic field in a spherical shell is described by a system of mean-field equations [13] (see also [14])

$$\begin{aligned} \frac{\partial A}{\partial t} &= \alpha B + \hat{L}A, \\ \frac{\partial B}{\partial t} &= -\Omega\frac{\partial}{\partial\theta}A + \hat{L}B, \end{aligned} \qquad (1)$$

where A and B are the azimuthal components of the vector potential $\mathbf{A}$ and the magnetic field $\mathbf{B} = \mathrm{curl}\mathbf{A}$, respectively; $\alpha(\theta)$ is the α-effect, $\Omega(\theta)$ is the differential rotation, $\hat{L} = \eta\left(\frac{1}{\sin\theta}\frac{\partial}{\partial\theta}\sin\theta\frac{\partial}{\partial\theta} - \frac{1}{\sin^2\theta}\right)$ is the diffusion operator, and η is the magnetic diffusion coefficient. System (1) is solved in the interval $0 \le \theta \le \pi$ with the boundary conditions $B = 0$ and $A = 0$ for $\theta = 0$ and π.

In the dynamo theory, the poloidal and toroidal components of the magnetic field are often used. In our case, the radial component of the magnetic field $B_r = \frac{1}{\sin\theta}\frac{\partial}{\partial\theta}(\sin\theta A)$ and the azimuthal one determine the poloidal and toroidal components, respectively.

The energy sources in system (1) are the α- and Ω-effects. The first is responsible for generating the poloidal component of the magnetic field from the toroidal one via turbulence. The second effect describes the generation of the toroidal component of the magnetic field due to the differential rotation of liquid.

The influence of the magnetic field on the flow (the nonlinearity) is specified by the algebraic α-quenching

$$\alpha(\theta) = \frac{\alpha_0(\theta)}{1 + E_m}, \qquad (2)$$

where $E_m(\theta) = (B_r^2 + B^2)/2$ is the magnetic energy.

2. THE INVERSE PROBLEM

The solution of the direct problem (1) and (2) with the prescribed profiles of $\alpha_0(\theta)$ and $\Omega(\theta)$ yields the field $\mathbf{B}(\theta, \mathbf{t})$ that can be compared to observations. One of the difficulties of such an approach is a poor knowledge of $\alpha_0(\theta)$ and $\Omega(\theta)$. As an example, in the planetary dynamo, these profiles are known only from the three-dimensional calculations. For the solar dynamo (see, e.g., [15]), the information on the differential rotation Ω is known from helioseismology, while the α-effect profiles vary from model to model. In the galactic dynamo, the situation is close to that of the solar dynamo, which causes the use of rather simple mean-field models. The above reasons motivate the approach where the profiles of the $\alpha_0(\theta)$- and $\Omega(\theta)$-effects would yield the solution $\mathbf{B}(\theta, \mathbf{t})$ that satisfies the specified properties, i.e., the solution of the inverse problem for system (1) and (2) (see [12]).

Let us introduce the cost function $\Psi(\mathbf{B}, \mathbf{B^0})$, where $\mathbf{B}$ and $\mathbf{B^0}$ are the modeled and observed magnetic fields, respectively. The function $\boldsymbol{\Psi}$ has at least one minimum at $\mathbf{B} = \mathbf{B^0}$. A proper choice of Ψ and, in general, the observed derivatives of the magnetic field $\mathbf{B^0}$ allow the problem to be reduced to searching for the global minimum. However, in practice, the observations do not cover the entire spatial domain of the magnetic-field generation, i.e., the problem turns out to be ill-defined. At the same time, the solution characteristics that are used in the comparison of the model solution to the observations may result in a large number of solutions with the same Ψ, i.e., the nonuniqueness of the solution. This means that the problem reduces to searching for the smallest Ψ under a large number of local minima, which, in turn, imposes some restrictions on the minimization algorithms [16].

The next step is to consider only the large-scale $\alpha_0(\theta)$ and $\Omega(\theta)$ profiles, which corresponds to the first N_α and N_Ω Fourier modes in the series over θ

$$\alpha_0 = \sum_{n=1}^{N_\alpha} C_n^\alpha \sin(2\theta n), \quad \Omega = \sum_{n=0}^{N_\Omega} C_n^\Omega \cos(2\theta n). \qquad (3)$$

The values of the magnetic energy and the equatorial asymmetry

n	N/S	E_m^P	E_m^T	E_m	η^P	η^T	η
	N	3	298	301			
I					0.33	1.60	1.54
	S	9	186	195			
	N	6	1	7			
II					0.99	0.04	0.22
	S	6	28	34			
	N	6	25	31			
III					1.60	15.8	5.85
	S	4	2	6			

The minimization problem will then be reduced to the search for such $\mathbf{C}^\alpha$ and $\mathbf{C}^\Omega$ that $\mathbf{\Psi}(\mathbf{C}^\alpha, \mathbf{C}^\Omega)$ has a minimum (probably, a local one). This is the minimization problem in the space of $d = N_\alpha + N_\Omega + 1$ dimensions. We note that to search for the minimum is not our goal in itself. In other words, our concern is the set of solutions at small $\mathbf{\Psi}$ rather than only a global minimum that may even be absent. The analysis of the $\alpha_0(\theta)$ and $\Omega(\theta)$ profiles for such solutions provides another insight into the model and observations. This is a good way of learning how to put questions to the model and to use it afterwards.

To solve the direct problem (1) and (2), we use the central second-order differences for approximating the spatial derivatives and the fourth-order Runge–Kutta method for integrating in time. The C++ code was developed for parallel computations with the MPI system, so that each computer node solved Eqs. (1) and (2) for a set of coefficients $(\mathbf{C}^\alpha, \mathbf{C}^\Omega)$ specified by the random-number Gaussian generator in a certain given range. To accelerate the convergence, the random distribution for $(\mathbf{C}^\alpha, \mathbf{C}^\Omega)$ was specified in such a way that the mean value was chosen to be equal to the best previous choice (i.e., corresponding to the minimum Ψ) for the particular coefficient. The dispersion was calculated with the 3σ rule, so that the entire interval was covered. This method is based on the Monte-Carlo technique [16] and turned out to be weakly sensitive to the presence of local minima in the cost function.

In the cluster computations, we used $N = 101$ grid points in θ space, a time step of $\tau = 10^{-5}$, and computer nodes $\mathcal{N}$ ranging from 10 to 100. The number of iterations was usually less than 10. The integration over time was performed for the interval $t = 20$. For the considered one-dimensional problem, the use of the cluster was not crucial, but this method can be easily developed for the multidimensional problem, where the need for parallel computations will be large.

Further, we will consider some particular forms of the cost function Ψ and discuss the meaning of the obtained $\alpha_0(\theta)$ and $\Omega(\theta)$ profiles.

3. MODEL RESULTS

The amplitude of the energy sources in Eq. (1) can be expressed by a single parameter, that is, the dynamo number $\mathcal{D} = \dfrac{\|a_0\| \, \|\Omega\| L^3}{\eta^2}$, where $L = \pi$ is the spatial scale and $\|\cdot\|$ is the norm. Here, we consider how the solution of system (1) and (2) with limited $\|\alpha_0\| \le \mathcal{D}_\alpha$ and $\|\Omega\| \le \mathcal{D}_\omega$ (where $\mathcal{D}_\alpha$ and $\mathcal{D}_\omega$ are constants) depends on the forms of the α_0 and Ω profiles. The choice of a particular form of the norm is rather arbitrary. Having in mind that α_0 is asymmetric relative to the equator, we will use the following definition: $\|f\| = \pi^{-1}\int_0^\pi |f| \sin\theta d\theta$.

The fact that the asymmetric magnetic field is present in Eqs. (1) and (2) was shown in [12], where the solutions with a nonzero flux of the magnetic field at the equator were considered. The dynamo waves passing through the equator on the Sun are a prototype of such a solution. The obtained solutions actually exhibited the equatorial asymmetry of the magnetic energy. Below, we will consider the cost functions that explicitly contain such asymmetry.

Let the ratio of the magnetic energies in the Northern (N) and Southern (S) hemispheres be η. We introduce the cost function as $\Psi = 1 - e^{-\mathcal{R}}$, where $\mathcal{R} = \min(\eta, \eta^{-1})$. The Ψ minimum corresponds to the highest ratio of the energies. Three cases will be considered: $\eta^P = \dfrac{E_m^{PN}}{E_m^{PS}}$ for the poloidal part (case I), $\eta^T = \dfrac{E_m^{TN}}{E_m^{TS}}$ for the toroidal part (case II), and $\eta = \dfrac{E_m^N}{E_m^S}$ for the total magnetic energy $E_m = E_m^P + E_m^T$ (case III).

The results of minimization of Ψ for Eq. (3) with $N_\alpha = N_\Omega = M$, $M = 3$, and $\mathcal{D} = 50$ are summarized in the table. The obtained solutions actually demonstrate a high degree of equatorial asymmetry in the magnetic energy distribution. This effect is strongest in case II, where $\eta^T = 0.04$, i.e., in the Southern hemisphere the magnetic energy of the toroidal component of the magnetic field is 25 times higher than that in the Northern one. For the poloidal component, $\mathbf{\Psi}$ is smallest for case I (as can be expected from the defini-

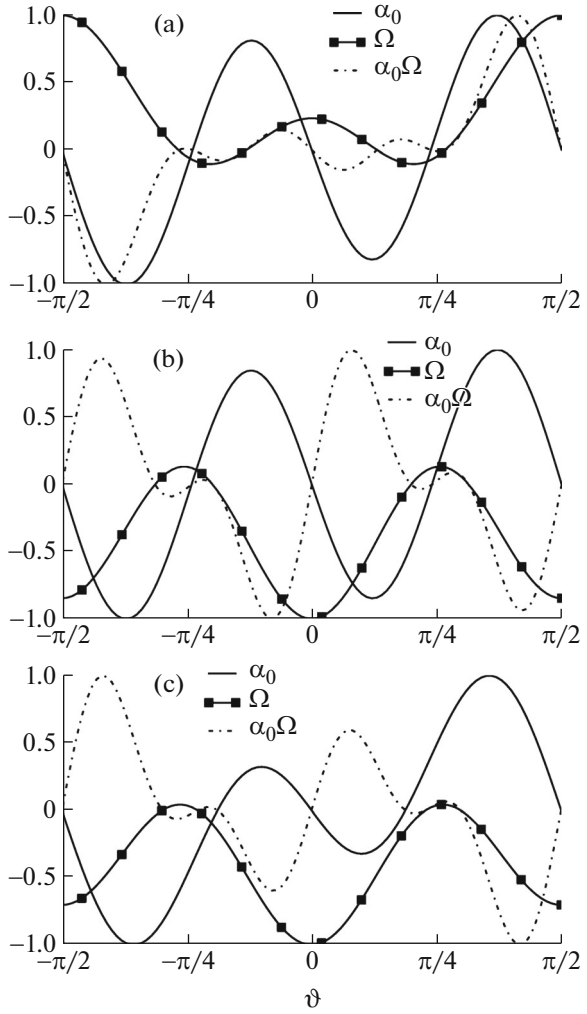

Fig. 1.

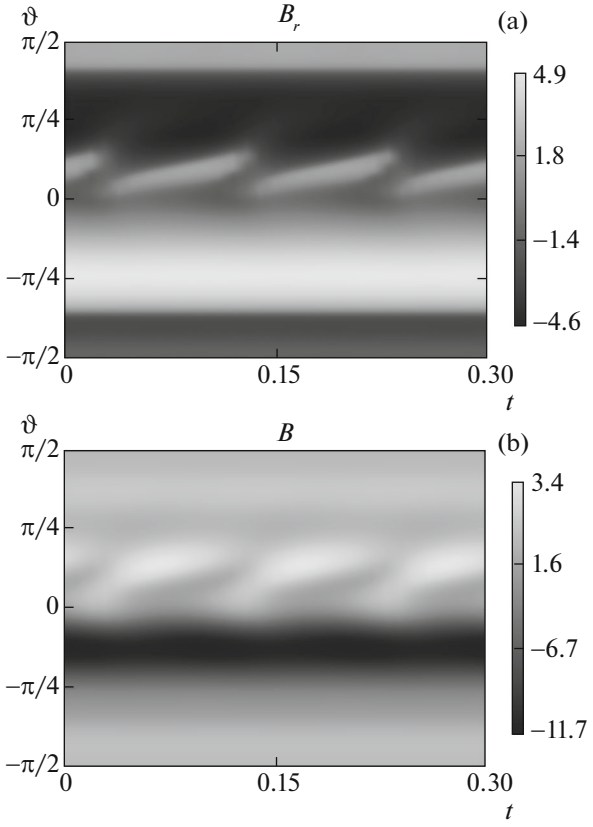

Fig. 2.

tion of **Ψ**). The results do not considerably depend on the Fourier-series length M.

To explain the causes of the equatorial asymmetry, let us consider the obtained α_0 and Ω profiles in more detail (Fig. 1). The analysis can be made in a simpler way if we take the fact into account that the solution of the linear problem (3) depends only of the product of the dynamo number $\mathcal{D} = \alpha_0 \cdot \Omega$ for the θ-independent values of α_0 and Ω. Since some features or the linear solution may be also present in the nonlinear mode, we show the product in Fig. 1 as well. The designation $\mathcal{D}$ will be also used for the case where it is not a number but a function of θ.

For case I, $\mathcal{D}$ shows an extremum at high latitudes, so that the zones of the maximum generation in the hemispheres that correspond to the extrema of $\mathcal{D}$ are widely spaced. This favors the isolation of the hemispheres from each other and, as a consequence, the increase of the probability of fields with different morphologies.

For case II, where the ratio of the toroidal energies is at a maximum, $\mathcal{D}$ shows two local extrema, one of which is very close to the pole. For case III, the situation is the same: the near-pole extremum is better expressed. The additional analysis of the solutions that contain no asymmetry also supports the influence of the distance between the extrema of the maximum generation in the hemispheres: for these modes the extrema were near the equator. At the equator itself, where α_0 changes sign, $\mathcal{D} = 0$.

In this connection, it is worth mentioning [17], where the transition zone from the symmetric dynamo mode to the asymmetrical one that also corresponds to widely spaced extrema of the maximum generation was found from linear analysis. However, it should be noted that the analysis was made under the conditions that α_0 may contain the Fourier modes symmetrical relative to the equator, which contradicts the physical concept of this quantity.

Along with the concept of isolation of the generation sources in different hemispheres, the explanation of the asymmetry due to superposition of the dipole and quadrupole modes is also widely accepted. To verify this hypothesis, we expanded the B_r and B field

components in the Legendre polynomials. Selection of the comparable amplitudes results in the following. For case I, they are modes (1, 2, 3) and (1, 2) for the poloidal and toroidal field, respectively. Here, the numbers mean a dipole (1), a quadrupole (2), and so on. This case is generally consistent with the concept of the dipole and quadrupole superposition inducing asymmetry.

The situation for cases II and III is different: at least five first modes are responsible for the asymmetry. There is no doubt that the observed asymmetry results from the superposition of even and odd modes, although because of their large number. The larger their number is, the higher the accuracy is with which the stepwise distribution of the field with a sudden change at the equator can be obtained, and the higher the degree of equatorial asymmetry will be. It is clear that such a scenario can occur if there is a correlation between the modes, although this condition may be violated under large M due to turbulent effects.

We have not discussed the temporal behavior of the fields. The solution is stationary for cases I and III, while it is periodic for case II. It would be provocative to compare case II to the solar dynamo, where the asymmetry of magnetic activity occurred during the Maunder minimum [5]. However, this scenario does not work, because the dynamo waves are directed from the equator to the poles (Fig. 2) rather than the reverse, as on the Sun. This corresponds to the opposite sign of $\mathcal{D}$. The tests with the other sign of $\mathcal{D}$ failed to yield an asymmetric solution. It is also worth noting that the oscillating component in the obtained solutions is much smaller than the stationary one. The dynamic α-quenching model was also tested in numerical experiments [18]. We managed to obtain an equatorward dynamo wave, although the degree of asymmetry was negligible.

CONCLUSIONS

Usually, dynamo modeling is reduced to solving the direct problem with specified parameters. However, even Parker's one-dimensional model with algebraic quenching turns out to be so sensitive to the choice of the parameters that there is no guarantee of the correctness of the comparison of the results with the observations. Moreover, in many cases, the parameters themselves are to be determined. Due to these issues, the entire configuration space of the model should be analyzed. However, this may be a challenging problem for more complex systems than those considered above. In this connection, searching for the optimal solution and developing the corresponding algorithms are more promising. For this purpose, the above-discussed method for solving the inverse problem can be used. What is more important, this method provides a new insight into the model. By formulating different requirements for the solution, which can be summed with different weights, one can better understand the properties of the model.

Turning to the phenomenon of the equatorial asymmetry considered above, we should note how our results relate to those of the three-dimensional modeling mentioned in the Introduction. According to [8], the asymmetry in the magnetic field weakly influences the flow asymmetry, at least at the level of the amplitudes of the kinetic energy in the hemispheres. In the above model, the α-effect is quenched due to the local increase of the magnetic energy. In other words, the magnetic energy correlates with the α-effect amplitude. From the considered mean-field model, it is not clear how this phenomenon is connected with the changes in the kinetic energies themselves; more sophisticated models, taking hydrodynamic effects into account, should be applied. It is also good to bear in mind that the dynamo theory often deals with forceless modes, when the magnetic field energy is large and the electric current direction is close to that of the magnetic field. In this case, the arising Lorentz force, whose effect on the flow is opposite, will be weak and the magnetic field may accumulate great energy. Such a situation takes place in a geodynamo. It is evident that the mechanism that quenches the generation sources of the magnetic field should be modified for such systems.

ACKNOWLEDGMENTS

This study was supported by the Russian Science Foundation (project no. 16-17-10097).

REFERENCES

1. A. A. Ruzmaikin, A. M. Shukurov, and D. D. Sokoloff, *Magnetic Fields of Galaxies* (Springer, 1988). doi 10.1007/978-94-009-2835-0
2. G. Rüdiger, L. L. Kitchatinov, and R. Hollerbach, *Magnetic Processes in Astrophysics: Theory, Simulations, Experiments* (Wiley, 2013). doi 10.1002/9783527648924
3. D. Gubbins, C. N. Barber, S. Gibbons, and J. J. Love, Proc. R. Soc. A **456**, 1669 (2000). doi 10.1098/rspa.2000.0581
4. R. Knaack, J. O. Stenflo, and S. V. Berdyugina, Astron. Astrophys. **418**, L17 (2004). doi 10.1051/0004-6361:20040107
5. J. C. Ribes and E. Nesme-Ribes, Astron. Astrophys. **276**, 549 (1993).
6. S. Stanley, L. Elkins-Tanton, M. T. Zuber, and E. M. Parmentier, Science **321**, 1822 (2008). doi 10.1126/science.1161119
7. E. Grote and F. H. Busse, Phys. Rev. E **62**, 4457 (2000). doi 10.1103/PhysRevE.62.4457
8. F. H. Busse and R. D. Simitev, Geophys. Astrophys. Fluid Dyn. **100**, 341 (2006). doi 10.1080/03091920600784873

9. M. Landeau and J. Aubert, Phys. Earth Planet. Inter. **185**, 61 (2011). doi 10.1016/j.pepi.2011.01.004
10. H. Amit, U. R. Christensen, and B. Langlais, Phys. Earth Planet. Inter. **189**, 63 (2011). doi 10.1016/j.pepi.2011.07.008
11. W. Dietrich and J. Wicht, Phys. Earth Planet. Inter. **217**, 10 (2013). doi 10.1016/j.pepi.2013.01.001
12. M. Yu. Reshetnyak, Russ. J. Earth Sci. **15**, ES4001 (2015). doi doi 10.2205/2015ES000558
13. E. N. Parker, Astrophys. J. **122**, 293 (1955). doi 10.1086/146087
14. M. Stix, *The Sun: An introduction* (Springer, 1989). doi 10.1007/978-3-642-56042-2
15. G. Belvedere, K. Kuzanyan, and D. D. Sokoloff, Mon. Not. R. Astron. Soc. **315**, 778 (2000). doi 10.1046/j.1365-8711.2000.03458.x
16. W. H. Press, S. A. Teukolsky, W. T. Vetterling, and B. P. Flannery, *Numerical Recipes. The Art of Scientific Computing*, 3rd ed. (Cambridge Univ. Press, 2007)
17. B. Gallet and F. Pétrélis, Phys. Rev. E **80**, 035302 (2009). doi 10.1103/PhysRevE.80.035302
18. N. Kleeorin, I. Rogachevskii, and A. Ruzmaikin, Astron. Astrophys. **297**, 159 (1995).

Translated by E. Petrova